Analysis of Electromagnetic Wave Propagation in Frequency Bands of Nonlinear Metamaterials

Nikolaos L. Tsitsas

Department of Informatics,
Aristotle University of Thessaloniki, 54124 Thessaloniki, Greece
ntsitsas@csd.auth.gr

Abstract — Electromagnetic wave propagation phenomena in nonlinear metamaterials are investigated for waves propagating either in the left-handed frequency band or in the frequency band gaps. In the left-handed band, we implement directly the reductive perturbation method to Faraday's and Ampére's laws and derive a second-and a third-order nonlinear Schrödinger (NLS) equation, describing solitons of moderate and ultra-short pulse widths, respectively. Then, we find necessary conditions and derive exact bright and dark soliton solutions of these equations. On the other hand, in the frequency band gaps with negative linear effective permittivity and positive permeability (where linear electromagnetic waves are evanescent), we derive two short-pulse equations (SPEs) for the high- and low-frequency band gaps. The structure of the SPEs solutions is discussed, and connections with the NLS soliton solutions are presented. Numerical simulations of the SPEs solutions are included and compared with those of the reduced wave equations. Directions towards the modelling of wave propagation in nonlinear chiral metamaterials are pointed out.

Index Terms — Frequency band gaps, left-handed media, negative refractive index, nonlinear metamaterials, nonlinear Schrödinger equations, ultra-short pulses.

I. INTRODUCTION

The remarkable electromagnetic (EM) properties and numerous potential applications of metamaterials (MMs) have been meticulously documented in the literature (see e.g. the classic books [1,2]. By considering a Drude model for the effective permittivity ϵ and a Lorentz model for the magnetic permeability μ of the MM, it is seen that there exist three different types of frequency bands in the MM: (i) those displaying a right-handed (RH) behavior characterized by $\epsilon > 0$, $\mu > 0$, or (ii) a left-handed (LH) behavior characterized by $\epsilon < 0$, $\mu < 0$, and thus exhibiting negative refractive index, or (iii) frequency band gaps, namely domains where linear EM waves are evanescent, e.g., for $\epsilon < 0$ and $\mu > 0$. Each of the above bands exhibits significantly different properties referring to the associated propagation and localization of EM waves. The RH band has been extensively analyzed; here, we focus on waves propagating either in the LH regime or in the band gaps.

Concerning first LH MMs, they exhibit negative refractive index at the microwave [3-5] as well as at the optical frequencies [6], and hence they are characterized by unique properties, including: reversal of Snell's law, backward wave propagation, reversal of the Doppler shift and Cherenkov effect, collecting lens behavior forming 3-D images, perfect lens performance, and so on [7,8]. To this end, they have become a subject of intense research activity; see the reviews [9-12]. Such MMs are experimentally realized mainly by periodic arrays of thin conducting wires, exhibiting plasma behavior, and split-ring resonators (SRR's), resembling parallel plate capacitors, generating negative ϵ and μ, respectively [3,4]. For other realizations of LH MMs and related discussions see [13-15].

So far, MMs have been mainly investigated in the linear regime, where ϵ and μ are independent of the EM fields intensities. Nevertheless, *nonlinear* MMs, which may be created by embedding an array of wires and SRR's into a nonlinear dielectric [16,17], are useful in various applications. In particular, it has been demonstrated that the field intensity acts as a control mechanism, altering the MM properties from LH to RH and back. Hence, the study of MMs nonlinear properties may assist in the implementation of tunable structures with intensity controlled transmission and in studying nonlinear effects in negative refraction photonic

Submitted On: Oct. 12, 2011
Accepted On: Jan. 26, 2012

crystals. Furthermore, it was shown in [18] that LH weakly nonlinear MMs support propagation of vector solitons.

On the other hand, concerning the frequency band gaps, they are characterized by $\epsilon < 0$ and $\mu > 0$ and hence linear EM waves are evanescent. In particular, there exist two band gaps which will be named as the "low-frequency" (LF) and the "high-frequency" (HF) gap. However, when a nonlinearity occurs, e.g. in the dielectric response of the MM [16-22], then nonlinearity-induced localization of EM waves is possible. Such localization is indicated by the formation of *gap solitons*, occurring mainly in nonlinear optics [23]. Gap solitons were also predicted in nonlinear MMs as solutions of a nonlinear Klein-Gordon equation [24].

In this work, first we analyze EM wave propagation in nonlinear lossy LH MMs. The methodology consists in starting from the Maxwell's equations, and using the reductive perturbation method to derive systematically a nonlinear Schrödinger (NLS) equation and a higher-order NLS (HNLS) equation for the EM fields envelopes, governing the propagation of ultra-short solitons. Analyzing the NLS and HNLS equations, we find necessary conditions for the formation of bright or dark solitons in the LH regime, and derive exact ultra-short solitons propagating in nonlinear LH MMs. The developed direct analysis of the Maxwell's equations, rather than the coupled wave equations for the EM fields envelopes, shows that the electric field envelope is proportional to the magnetic field one (their ratio being the linear wave-impedance). Thus, for each of the EM wave components, we derive a *single* NLS (for moderate pulse widths) or a *single* HNLS equation (for ultra-short pulse widths), rather than a system of *coupled* NLS equations (as in existing literature, see e.g. [18]). The HNLS equation, which incorporates higher-order dispersive and nonlinear terms, generalizes the one describing short pulse propagation in nonlinear optical fibers.

Then, we proceed with the analysis of nonlinear localized EM waves propagating in the frequency band gaps of nonlinear MMs. More precisely, we derive nonlinear evolution equations describing *ultra-short* pulses (possessing pulse widths of the order of a few cycles of the carrier frequency) that can be formed in these band gaps. In doing so, we consider a MM characterized by the permittivity ϵ and permeability μ of [3], as well as a weak Kerr-type nonlinearity in its dielectric response [20,21,24]. By modifying the techniques of [25,26], we derive appropriate expressions for μ in the HF and LF band gaps. Then, we use a multiscale perturbation method, with different small parameters for the HF and LF gaps depending on the MM characteristics, to derive from Maxwell's equations two *short-pulse equations* SPEs. Each of these equations describes the evolution of ultra-short pulses either in the HF or the LF gap. The SPE has been shown to be the proper model for describing the evolution of ultra-short pulses in nonlinear fiber optics [25]; moreover in [25] the solutions of Maxwell's equations were compared numerically to the ones of the SPE and NLS models and it was shown that the accuracy of the SPE (NLS) increases (decreases) as the pulse width shortens. We also discuss the structure of the resulting peakon-like solutions of the SPEs derived in our context of nonlinear MMs, and draw parallels to NLS-like soliton solutions (which can be regarded as ultra-short gap solitons in nonlinear MMs). Numerical simulations of the peakon-like and breather-like solutions are also included both in the context of the SPEs as well as in that of the reduced wave equations originating from Maxwell's equations.

Investigations of the above described phenomena were initiated in [27] and [28]. This paper contains a unified treatment of these investigations, provides appropriate extensions and points out generalizations concerning the modelling of wave propagation in more complicated types of nonlinear MMs (e.g. chiral MMs).

II. DESCRIPTION OF THE NONLINEAR METAMATERIAL

We consider a composite lossy nonlinear MM, consisting of an array of conducting wires and SRRs, with the slits of the SRRs filled with a weakly nonlinear dielectric [16,18-20,22]. The MM is characterized by a frequency dependent effective complex permittivity $\hat{\epsilon}(\omega)$ and magnetic permeability $\hat{\mu}(\omega)$ (below f and $\hat{f}$ denote any function f in the time- and frequency-domain, respectively) given by [3,16]:

$$\hat{\epsilon}(\omega; |\mathbf{E}|^2) = \epsilon_0 \left(\epsilon_D(|\mathbf{E}|^2) - \frac{\omega_p^2}{\omega^2 + i\omega\gamma_\epsilon} \right),$$

$$\hat{\mu}(\omega; |\mathbf{H}|^2) = \mu_0 \left(1 - \frac{F\omega^2}{\omega^2 + i\omega\gamma_\mu - \omega_{0NL}^2(|\mathbf{H}|^2)} \right),$$

where ϵ_0 and μ_0 are the vacuum permittivity and permeability, ω is the EM wave's frequency, ω_p is the plasma frequency, F is the filling factor, γ_ϵ and γ_μ are the linear loss frequencies, ω_{0NL} is the nonlinear resonant SRR frequency [16], $\mathbf{E}$ and $\mathbf{H}$

are the electric and magnetic field intensities. In the linear limit, $\epsilon_D \to 1$ and $\omega_{0NL} \to \omega_{\rm res}$ ($\omega_{\rm res}$ is the linear resonant SRR frequency).

In particular, we assume the decompositions [18-22,29]:

$$\hat{\epsilon}(\omega;|\mathbf{E}|^2) = \hat{\epsilon}_L(\omega) + \epsilon_{NL}(|\mathbf{E}|^2), \quad (1)$$

$$\hat{\mu}(\omega;|\mathbf{H}|^2) = \hat{\mu}_L(\omega) + \mu_{NL}(|\mathbf{H}|^2). \quad (2)$$

For the linear parts we assume a Drude (Lorentz) model for the permittivity (permeability) [27]:

$$\hat{\epsilon}_L(\omega) = \epsilon_0\left(1 - \frac{\omega_p^2}{\omega^2 + i\omega\gamma_\epsilon}\right), \quad (3)$$

$$\hat{\mu}_L(\omega) = \mu_0\left(1 - \frac{F\omega^2}{\omega^2 + i\omega\gamma_\mu - \omega_{\rm res}^2}\right), \quad (4)$$

while the weakly nonlinear parts of the permittivity and permeability exhibit a Kerr-type behavior and are, respectively, given by [18-22]:

$$\epsilon_{NL}(|\mathbf{E}|^2) = \epsilon_0\alpha|\mathbf{E}|^2, \quad (5)$$

$$\mu_{NL}(|\mathbf{H}|^2) = \mu_0\beta|\mathbf{H}|^2, \quad (6)$$

where α and β are the Kerr coefficients; $\alpha > 0$ and $\alpha < 0$ corresponds to focusing and defocusing dielectrics.

Assuming that $\omega_p > \omega_{\rm res}$ and that the linear losses γ_ϵ and γ_μ are small compared to the operating frequency, the dispersion relation $k_0^2 = \omega_0^2{\rm Re}[\hat{\epsilon}_L(\omega_0)]{\rm Re}[\hat{\mu}_L(\omega_0)]$ (k_0 the wavenumber corresponding to the carrier frequency ω_0) shows that linear waves exist ($k_0^2 > 0$) in the bands $\omega > \omega_p$ and $\omega_{\rm res} < \omega < \omega_M \equiv \omega_{\rm res}/\sqrt{1-F}$, where the medium is right-handed (RH) and left-handed (LH), respectively. These bands will be called the RH and LH bands. On the other hand, there exist two bands, with ${\rm Re}[\hat{\epsilon}_L] < 0$ and ${\rm Re}[\hat{\mu}_L] > 0$, where linear waves are evanescent ($k_0^2 < 0$). These "band-gaps" are $0 < \omega < \omega_{\rm res}$ ["low-frequency" (LF) gap], and $\omega_M < \omega < \omega_p$ ["high-frequency" (HF) gap]. Typical dispersion curves of ${\rm Re}[\hat{\epsilon}_L](\omega)$ and ${\rm Re}[\hat{\mu}_L](\omega)$ are shown in Fig. 1.

In the sequel, we consider the physically relevant [18] values of parameters: $F = 0.4$, $\omega_{\rm res} = 2\pi \times 1.45$ GHz, $\omega_M = 2\pi \times 1.87$ GHz, and $\omega_p = 2\pi \times 10$ GHz, for which α may be positive or negative, while β is positive.

III. EM WAVE PROPAGATION IN THE LEFT-HANDED BAND

First, we analyze the frequency band $2\pi \times 1.45$ GHz $< \omega < 2\pi \times 1.87$ GHz, inside which the SRRs are negative-index LH media (with ${\rm Re}[\hat{\epsilon}_L] < 0$ and ${\rm Re}[\hat{\mu}_L] < 0$), as was discussed above.

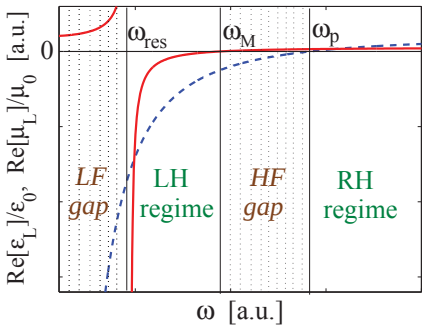

Fig. 1. ${\rm Re}[\hat{\mu}_L]/\mu_0$ [solid (red) line], and ${\rm Re}[\hat{\epsilon}_L]/\epsilon_0$ [dashed (blue) line] versus ω in arbitrary units (a.u.). Linear waves propagate (${\rm Re}[\hat{\epsilon}_L]{\rm Re}[\hat{\mu}_L] > 0$) for $\omega > \omega_p$ (RH regime) and $\omega_{\rm res} < \omega < \omega_M$ (LH regime). Dotted regions with ${\rm Re}[\hat{\epsilon}_L] < 0$ and ${\rm Re}[\hat{\mu}_L] > 0$ depict the LF gap ($0 < \omega < \omega_{\rm res}$) and the HF gap ($\omega_M < \omega < \omega_p$).

A. Propagation along the $+\hat{\mathbf{z}}$ axis

We consider the propagation along the $+\hat{\mathbf{z}}$ direction of a x- (y-) polarized electric (magnetic) field, namely,

$$\mathbf{E}(z,t) = \hat{\mathbf{x}}E(z,t) \quad , \quad \mathbf{H}(z,t) = \hat{\mathbf{y}}H(z,t). \quad (7)$$

Then, using the constitutive relations (in frequency domain) $\hat{\mathbf{D}}$=$\hat{\epsilon}\hat{\mathbf{E}}$ and $\hat{\mathbf{B}}$=$\hat{\mu}\hat{\mathbf{H}}$ ($\hat{\mathbf{D}}$ and $\hat{\mathbf{B}}$ are the electric flux density and the magnetic induction), Faraday's and Ampére's laws respectively read (in the time domain):

$$\partial_z E = -\partial_t(\mu * H), \quad \partial_z H = -\partial_t(\epsilon * E), \quad (8)$$

where $*$ denotes the convolution integral, i.e., $f(t)*g(t) = \int_{-\infty}^{+\infty} f(\tau)g(t-\tau)d\tau$, for functions $f(t)$ and $g(t)$.

Note that Eqs. (8) may be used in either the RH or the LH regime of a MM: once the dispersion relation $k_0 = k_0(\omega_0)$ and the evolution equations for the fields E and H are found, then $k_0 > 0$ ($k_0 < 0$) corresponds to the RH (LH) regime. Alternatively, for fixed $k_0 > 0$, one should shift the fields as $[E,H]^T \to [\pm E, \mp H]^T$ (either up or down sign combinations), thus inverting the orientation of the magnetic field and associated Poynting vector. Below, in our consideration we will assume that the wavenumber $k_0 = k_0(\omega_0)$ obtained from the linear dispersion relation [see Eq. (20) below] will be $k_0 < 0$ for the LH regime.

Next, we consider that:

$$[E(z,t), H(z,t)]^T = [q(z,t), p(z,t)]^T e^{i(k_0 z - \omega_0 t)}, \quad (9)$$

where q and p are the unknown EM fields envelopes.

B. Nonlinear evolution equations by the reductive perturbation method

Nonlinear evolution equations for the field envelopes can be found by the *reductive perturbation method* [30] as follows. First, we assume that the temporal spectral width of the nonlinear term with respect to the spectral width of the quasi-plane-wave dispersion relation is characterized by the formal small parameter ε [31,32].

Then, we introduce the slow variables:

$$Z = \varepsilon^2 z, \qquad T = \varepsilon(t - k_0' z), \tag{10}$$

where $k_0' \equiv v_g^{-1}$ is the inverse of the group velocity (hereafter, primes will denote derivatives with respect to ω_0). Additionally, we express q and p as asymptotic expansions in terms of ε,

$$q(Z,T) = q_0(Z,T) + \varepsilon q_1(Z,T) + \varepsilon^2 q_2(Z,T) + \cdots \tag{11}$$

$$p(Z,T) = p_0(Z,T) + \varepsilon p_1(Z,T) + \varepsilon^2 p_2(Z,T) + \cdots$$

and assume that the Kerr coefficients α and β are of order $\mathcal{O}(\varepsilon^2)$ (see, e.g., [18,31] as well as [33,34]). Moreover, the linear components of $\hat{\epsilon}_L$ and $\hat{\mu}_L$ are decomposed into real and imaginary parts, as follows:

$$\hat{\epsilon}_L(\omega) = \hat{\epsilon}_R(\omega) - i\hat{\epsilon}_I(\omega), \tag{12}$$

$$\hat{\mu}_L(\omega) = \hat{\mu}_R(\omega) - i\hat{\mu}_I(\omega), \tag{13}$$

where the imaginary parts are assumed to be $\mathcal{O}(\varepsilon^2)$. Note that the effect of losses in $\hat{\epsilon}_L$ and $\hat{\mu}_L$ is taken here for the first time into account since the analysis of [27] concerns the lossless case.

Then, substituting Eqs. (11) into Eqs. (8), using Eqs. (1), (2), and (10), and Taylor expanding $\hat{\epsilon}_L$, and $\hat{\mu}_L$, we arrive at the following hierarchy of equations:

$$\mathcal{O}(\varepsilon^0): \ \mathbf{W}\mathbf{x}_0 = \mathbf{0}, \tag{14}$$

$$\mathcal{O}(\varepsilon^1): \ \mathbf{W}\mathbf{x}_1 = -i\mathbf{W}'\partial_T \mathbf{x}_0, \tag{15}$$

$$\mathcal{O}(\varepsilon^2): \ \mathbf{W}\mathbf{x}_2 = -i\mathbf{W}'\partial_T \mathbf{x}_1 + \frac{1}{2}\mathbf{W}''\partial_T^2 \mathbf{x}_0 + \frac{k_0''}{2}\partial_T^2 \mathbf{x}_0 - i\partial_Z \mathbf{x}_0 - (\mathbf{A} - i\mathbf{B})\,\mathbf{x}_0, \tag{16}$$

$$\mathcal{O}(\varepsilon^3): \ \mathbf{W}\mathbf{x}_3 = -i\mathbf{W}'\partial_T \mathbf{x}_2 + \frac{1}{2}\mathbf{W}''\partial_T^2 \mathbf{x}_1 + \frac{i}{6}\mathbf{W}'''\partial_T^3 \mathbf{x}_0 + \frac{ik_0'''}{6}\partial_T^3 \mathbf{x}_0 + \frac{k_0''}{2}\partial_T^2 \mathbf{x}_1 - i\partial_Z \mathbf{x}_1 - (\mathbf{A} - i\mathbf{B})\,\mathbf{x}_1 - (\mathbf{B}'\partial_T - i\mathbf{C})\mathbf{x}_0, \tag{17}$$

with $\mathbf{x}_i = [q_i, p_i]^{\mathrm{T}}$ $(i = 0, 1, 2, 3)$ unknown vectors, and

$$\mathbf{W} = \begin{bmatrix} -k_0 & \omega_0\hat{\mu}_R \\ \omega_0\hat{\epsilon}_R & -k_0 \end{bmatrix}, \ \mathbf{A}\mathbf{x}_i = \omega_0 \begin{bmatrix} \beta|p_0|^2 p_i \\ \alpha|q_0|^2 q_i \end{bmatrix}$$

$$\mathbf{B} = \begin{bmatrix} 0 & \omega_0\hat{\mu}_I \\ \omega_0\hat{\epsilon}_I & 0 \end{bmatrix}, \tag{18}$$

$$\mathbf{C}\mathbf{x}_0 = \begin{bmatrix} -\beta\partial_T(|p_0|^2 p_0) + i\omega_0\beta(p_0 p_1^\star + p_0^\star p_1)p_0 \\ -\alpha\partial_T(|q_0|^2 q_0) + i\omega_0\alpha(q_0 q_1^\star + q_0^\star q_1)q_0 \end{bmatrix}$$

with $\star$ denoting complex conjugate.

The compatibility conditions required for the solvability of Eqs. (14)–(17) (known also as Fredholm alternatives [30,31]) are: $\mathbf{L}\mathbf{W}\mathbf{x}_i = 0$, where $\mathbf{L} = [1, \hat{Z}_L]$ is a left eigenvector of $\mathbf{W}$, such that $\mathbf{L}\mathbf{W} = \mathbf{0}$, and $\hat{Z}_L = \sqrt{\hat{\mu}_R/\hat{\epsilon}_R}$ is the linear wave-impedance, when dissipation is small enough to be ignored.

The leading-order Eq. (14) provides the following results. First, the solution $\mathbf{x}_0$ of Eq. (14) has the form:

$$\mathbf{x}_0 = \mathbf{R}\phi(Z,T), \tag{19}$$

where $\phi(Z,T)$ an under determination scalar field and $\mathbf{R} = [1, \hat{Z}_L^{-1}]^{\mathrm{T}}$ a right eigenvector of $\mathbf{W}$, such that $\mathbf{W}\mathbf{R} = \mathbf{0}$. Second, by using the compatibility condition $\mathbf{L}\mathbf{W}\mathbf{x}_0 = 0$ and Eq. (19), we obtain that $\mathbf{L}\mathbf{W}\mathbf{R} = 0$, which is actually the linear dispersion relation:

$$k_0^2 = \omega_0^2 \hat{\epsilon}_R \hat{\mu}_R, \tag{20}$$

with all functions of frequency evaluated at ω_0. Eq. (20) is also obtained by the nontrivial solution condition $\det\mathbf{W} = 0$. Third, the electric and magnetic field envelopes are proportional to each other, i.e. $q_0 = p_0\hat{Z}_L$.

Next, at $\mathcal{O}(\varepsilon^1)$, the compatibility condition for Eq. (15) results in $\mathbf{L}\mathbf{W}'\mathbf{R} = 0$, written as:

$$2k_0 k_0' = \omega_0^2(\hat{\epsilon}_R\hat{\mu}_R' + \hat{\epsilon}_R'\hat{\mu}_R) + 2\omega_0\hat{\epsilon}_R\hat{\mu}_R. \tag{21}$$

This is actually the definition of the group velocity $v_g = 1/k_0'$, as can also be found by differentiating the dispersion relation Eq. (20) with respect to ω. Furthermore, by combining Eqs. (15) and (19), we get that:

$$\mathbf{x}_1 = i\mathbf{R}'\partial_T\phi(Z,T) + \mathbf{R}\psi(Z,T), \tag{22}$$

where $\psi(Z,T)$ is an unknown scalar field. Next, at order $\mathcal{O}(\varepsilon^2)$, the compatibility condition for Eq. (16), combined with Eqs. (19) and (22), yields the following nonlinear Schrödinger (NLS) equation:

$$i\partial_Z\phi - \frac{1}{2}k_0''\partial_T^2\phi + \vartheta|\phi|^2\phi = i\tilde{g}\phi, \tag{23}$$

where k_0'' is the group-velocity dispersion coefficient, while $\tilde{g}$ and ϑ are, respectively, the linear loss and nonlinear coefficients which are given by:

$$\tilde{g} = \frac{k_0}{2\hat{\epsilon}_R\hat{\mu}_R}\left(\hat{\epsilon}_R\hat{\mu}_I + \hat{\mu}_R\hat{\epsilon}_I\right), \tag{24}$$

$$\vartheta = \frac{\omega_0^2}{2k_0}\left(\epsilon_0\alpha\hat{\mu}_R + \mu_0\beta\hat{\epsilon}_R\hat{Z}_L^{-2}\right). \tag{25}$$

Importantly, once ϕ is obtained from the NLS Eq. (23), the electric and magnetic field envelopes are, respectively, determined by means of Eq. (19) as $q_0 = \phi$ and $p_0 = \hat{Z}_L^{-1}\phi$, similarly to the case of a linear medium.

Finally, to order $\mathcal{O}(\varepsilon^3)$, we use the compatibility condition for Eq. (17), as well as Eqs. (16), (19), and (22), and obtain a NLS equation, incorporating higher-order dispersive and nonlinear terms. This equation describes the evolution of ψ, and yet contains ϕ, which obeys Eq. (23). By following [31] and [32], we introduce a new combined function $\Phi = \phi + \varepsilon\psi$, and then combine the NLS equations obtained at $\mathcal{O}(\varepsilon^2)$ and $\mathcal{O}(\varepsilon^3)$ to find that Φ obeys the higher-order NLS (HNLS) equation:

$$i\partial_Z\Phi - \frac{1}{2}k_0''\partial_T^2\Phi + \vartheta|\Phi|^2\Phi = i\varepsilon\left[\frac{1}{6}k_0'''\partial_T^3\Phi - \frac{\vartheta}{\omega_0}\partial_T(|\Phi|^2\Phi) + i\tilde{g}'\partial_T\Phi\right]. \tag{26}$$

For $\varepsilon = 0$, the HNLS Eq. (26) is reduced to the NLS Eq. (23), while for $\varepsilon \neq 0$ generalizes the HNLS equation describing ultra-short pulse propagation in optical fibers [31,32] (where $\mu = \mu_0$, while dispersion and nonlinearity appear solely in the fiber dielectric properties). As in the case of the NLS Eq. (23), Eq. (26) provides the field Φ which determines the electric and magnetic fields at $\mathcal{O}(\varepsilon^3)$, respectively, as $q_0 + \varepsilon q_1 = \Phi$ and $p_0 + \varepsilon p_1 = \hat{Z}_L^{-1}\Phi$ [see Eqs. (19) and (22)]. Note that Eqs. (23) or (26) can be used in the LH (RH) regime, taking k_0, $\hat{\epsilon}_R$, and $\hat{\mu}_R$ negative (positive), as per the discussion above.

In the sequel, we derive analytically exact soliton solutions of Eqs. (23) and (26).

C. Solitons solutions of the NLS equation

First, we analyze in detail the NLS Eq. (23): we start by measuring length, time, and the field intensity $|\phi|^2$ in units of the dispersion length $L_D = t_0^2/|k_0''|$, initial pulse width t_0, and $L_D/|\vartheta|$, respectively, and reduce Eq. (23) to the following dimensionless form:

$$i\partial_Z\phi - \frac{s}{2}\partial_T^2\phi + \sigma|\phi|^2\phi = ig\phi, \tag{27}$$

TABLE I: Conditions for the formation of bright or dark solitons (BS or DS) for the NLS Eq. (27)

		$s=+1$	$s=-1$
$\sigma=+1$	$\alpha>0$	DS	BS
$\sigma=-1$	$\alpha<0,\ \lvert\frac{\alpha}{\beta}\rvert > \frac{Z_0^2}{\hat{Z}_L^4}$	BS	DS
$\sigma=+1$	$\alpha<0,\ \lvert\frac{\alpha}{\beta}\rvert < \frac{Z_0^2}{\hat{Z}_L^4}$	DS	BS

where $s = \mathrm{sign}(k_0'')$, $\sigma = \mathrm{sign}(\vartheta)$, and $g = L_D\tilde{g}$. The NLS Eq. (27) admits bright (dark) soliton solutions for $s\sigma = -1$ ($s\sigma = +1$).

For our choice of parameters, numerical simulations indicate (see Fig. 2 of [27]) that inside the LH regime $s = +1$ ($k_0'' > 0$) for $2\pi \times 1.76 < \omega < 2\pi \times 1.87$ GHz, while $s = -1$ ($k_0'' < 0$) for $2\pi \times 1.45 < \omega < 2\pi \times 1.76$ GHz. On the other hand, the linear loss coefficient g attains very small values and can to a certain approximation be ignored. Moreover, regarding σ, it can take either the value $\sigma = +1$ or $\sigma = -1$, depending on the magnitudes and signs of the Kerr coefficients α and β. Note that we have assumed that $\beta > 0$, and hence $\sigma = +1$ either for a focusing dielectric, with $\alpha > 0$, or for a defocusing dielectric, $\alpha < 0$, with $|\alpha/\beta| < Z_0^2/\hat{Z}_L^4$ ($Z_0 = \sqrt{\mu_0/\epsilon_0}$ is the vacuum wave-impedance).

Thus, for $\sigma = +1$, bright (dark) solitons occur in the anomalous (normal) dispersion regimes, namely, for $k_0'' < 0$ ($k_0'' > 0$), respectively. On the other hand, $\sigma = -1$ for a defocusing dielectric ($\alpha < 0$), with $|\alpha/\beta| > Z_0^2/\hat{Z}_L^4$ and, bright (dark) solitons occur in the normal (anomalous) dispersion regimes. The above conclusions are summarized in Table I.

The "flexibility" due to the extra "degree of freedom" provided by the dispersion and nonlinearity properties of the magnetic response of the LH MM (missing in fiber optics), allows for the formation of bright (dark) solitons in the anomalous (normal) dispersion regimes for defocusing dielectrics (see third line of Table I).

D. Ultra-short solitons solutions of the HNLS equation

Now, we analyze the HNLS Eq. (26) which, by using the same dimensionless units as before, is expressed as:

$$i\partial_Z\Phi - \frac{s}{2}\partial_T^2\Phi + \sigma|\Phi|^2\Phi = i\delta_1\partial_T^3\Phi - i\sigma\delta_2\partial_T(|\Phi|^2\Phi) - \delta_3\partial_T\Phi, \tag{28}$$

where the coefficients δ_1, δ_2, and δ_3 are given by:

$$\delta_1 = \varepsilon \frac{k_0'''}{6t_0|k_0''|}, \quad \delta_2 = \varepsilon \frac{1}{\omega_0 t_0}, \quad \delta_3 = \varepsilon \frac{L_D \tilde{g}'}{t_0}. \tag{29}$$

Ultra-short solitons in nonlinear LH MMs can be predicted by means of Eq. (28). More precisely, following [35], and assuming negligible contribution from the linear losses (i.e. $\delta_3 \simeq 0$), we seek travelling-wave solutions of Eq. (28) of the form:

$$\Phi(Z,T) = U(\eta)\exp[i(KZ - \Omega T)], \tag{30}$$

where $U(\eta)$ is the unknown real envelope function, $\eta = T - \Lambda Z$, and the real parameters Λ, K, and Ω denote the wave's inverse velocity, wavenumber, and frequency. Substituting Eq. (30) into Eq. (28), the real and imaginary parts of the resulting equation read:

$$\ddot{U} + \frac{K - \frac{s}{2}\Omega^2 - \delta_1\Omega^3}{\frac{s}{2} + 3\delta_1\Omega} U - \frac{\sigma(1+\delta_2\Omega)}{\frac{s}{2} + 3\delta_1\Omega} U^3 = 0, \tag{31}$$

$$\delta_1 \dddot{U} + (\Lambda - s\Omega - 3\delta_1\Omega^2)\dot{U} - 3\sigma\delta_2 U^2 \dot{U} = 0, \tag{32}$$

where overdots denote differentiations with respect to η.

Notice that when $\delta_1 = \delta_2 = 0$, Eq. (32) is automatically satisfied if $\Lambda = s\Omega$ and the profile of "long" soliton pulses [governed by Eq. (27)] is determined by Eq. (31). On the other hand, for ultra-short solitons (corresponding to $\delta_1 \neq 0$, $\delta_2 \neq 0$), Eqs. (31) and (32) are consistent if:

$$\frac{K - \frac{s}{2}\Omega^2 - \delta_1\Omega^3}{\frac{s}{2} + 3\delta_1\Omega} = \frac{\Lambda - s\Omega - 3\delta_1\Omega^2}{\delta_1} \equiv \kappa, \tag{33}$$

$$-\frac{\sigma\delta_2}{\delta_1} = -\frac{\sigma(1+\delta_2\Omega)}{\frac{s}{2} + 3\delta_1\Omega} \equiv \nu, \tag{34}$$

where κ and ν are nonzero constants. In such a case, Eqs. (31) and (32) are equivalent to the equation of motion of the unforced and undamped Duffing oscillator:

$$\ddot{U} + \kappa U + \nu U^3 = 0. \tag{35}$$

For $\kappa\nu < 0$, Eq. (35) possesses two exponentially localized solutions [35], having the form of a hyperbolic secant (tangent) for $\kappa < 0$ and $\nu > 0$ ($\kappa > 0$ and $\nu < 0$), and thus corresponding to the bright, $U_{\rm BS}$ (dark, $U_{\rm DS}$) solitons of Eq. (28):

$$U_{\rm BS}(\eta) = (2|\kappa|/\nu)^{1/2}\,\mathrm{sech}(\sqrt{|\kappa|}\eta), \tag{36}$$

$$U_{\rm DS}(\eta) = (2\kappa/|\nu|)^{1/2}\tanh(\sqrt{\kappa/2}\eta). \tag{37}$$

These are *ultra-short* solitons of the HNLS Eq. (28), valid even for $\varepsilon = \mathcal{O}(1)$: since both δ_1, δ_2 of Eq. (28) scale as $\varepsilon(\omega_0 t_0)^{-1}$, it is clear that for $\omega_0 t_0 = \mathcal{O}(1)$, or for soliton widths $t_0 \sim \omega_0^{-1}$, the higher-order terms can be neglected and propagation is governed by Eq. (27). On the other hand, if $\omega_0 t_0 = \mathcal{O}(\varepsilon)$, the higher-order terms become important and solitons governed by the HNLS Eq. (28) are *ultra-short*, of width $t_0 \sim \varepsilon\omega_0^{-1}$, satisfying Faraday's and Ampére's laws in Eqs. (8) up to $\mathcal{O}(\varepsilon^3)$.

Concerning the condition for bright or dark soliton formation, namely $\kappa\nu < 0$, we note that κ depends on the free parameters K and Ω (and, thus, can be tuned on demand), while the parameter ν has the opposite sign from σ. This means that bright solitons are formed for $\kappa < 0$ and $\sigma = -1$ (i.e., $\alpha < 0$ with $|\alpha/\beta| > Z_0^2/\hat{Z}_L^4$), while dark ones are formed for $\kappa > 0$ and $\sigma = +1$ (i.e., $\alpha > 0$, or $\alpha < 0$ with $|\alpha/\beta| < Z_0^2/\hat{Z}_L^4$).

IV. EM WAVE PROPAGATION IN THE FREQUENCY BAND GAPS

Now, we consider the EM wave propagation in the two frequency band-gaps of the nonlinear MM (characterized by $\mathrm{Re}[\hat{\epsilon}_L] < 0$ and $\mathrm{Re}[\hat{\mu}_L] > 0$), where, as mentioned above, linear EM waves are evanescent ($k_0^2 < 0$). To this end, we assume that the MM exhibits a Kerr-type nonlinearity exclusively in its dielectric response, while the magnetic permeability is considered a linear function; this assumption is justified in [20,21,24].

As in (7), also here we assume propagation along the $+z$ direction of a x- (y-) polarized electric (magnetic) field. Then, Maxwell's equations lead to the following time-domain nonlinear wave equation for $E(z,t)$:

$$\partial_z^2 E - \partial_t^2(\epsilon_L * \mu_L * E) - \epsilon_0\alpha\partial_t^2(\mu_L * E^3) = 0. \tag{38}$$

Note that once the electric field $E(z,t)$ is obtained from Eq. (38), the magnetic field $H(z,t)$ is derived from Faraday's law.

In the sequel, we analyze the EM wave propagation separately in the "high-frequency" (HF) and "low-frequency" (LF) gaps. We assume that the MM is lossless; extensions to the lossy case are discussed in Sec. V below.

A. The high-frequency band gap

The HF band gap is defined by $\omega_M < \omega < \omega_p$ (see Fig. 1). In this regime, by assuming $\omega \gg \omega_{\rm res}$,

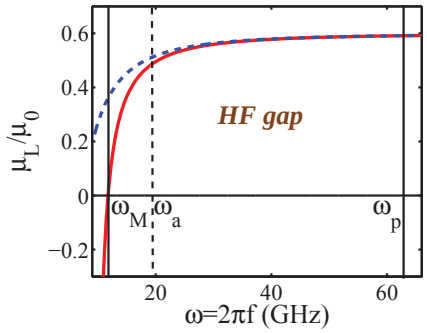

Fig. 2. Permeability $\hat{\mu}_L/\mu_0$ in the HF gap. Solid (red) and dashed (blue) lines correspond, respectively, to the exact [Eq. (4)] and approximate [Eq. (39)] expressions of $\hat{\mu}_L(\omega)/\mu_0$ in this band. The approximation produces a relative error less than 5% for $\omega_{\rm a} \equiv 2\pi \times 3.1$ GHz $< \omega < \omega_p = 2\pi \times 10$ GHz.

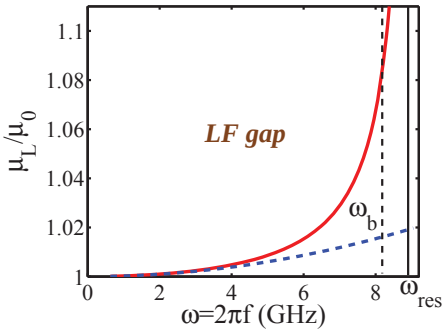

Fig. 3. Permeability $\hat{\mu}_L/\mu_0$ in the LF gap. Solid (red) and dashed (blue) lines correspond, respectively, to the exact [Eq. (4)], and approximate [Eq. (44)] expressions of $\hat{\mu}_L(\omega)/\mu_0$; a relative error of less than 5% is achieved for $\omega_{\rm b} \equiv 2\pi \times 1.28$ GHz $< \omega < \omega_{\rm res} = 2\pi \times 1.45$ GHz.

we find that $\hat{\mu}_L(\omega)$ in Eq. (4) is approximated by:

$$\hat{\mu}_L(\omega) \approx \mu_0(1-F) - \mu_0 F \frac{\omega_{\rm res}^2}{\omega^2}. \qquad (39)$$

Using the parameter values discussed above (namely $F = 0.4$, $\omega_{\rm res} = 2\pi \times 1.45$ GHz, $\omega_M = 2\pi \times 1.87$ GHz, and $\omega_p = 2\pi \times 10$ GHz), in Fig. 2 we show the exact [Eq. (4)] and approximate [Eq. (39)] expressions for the effective permeability in this band. As seen, in Fig. 2, the above approximation produces a relative error from the exact form of $\hat{\mu}_L(\omega)/\mu_0$ less than 5% in a wide sub-interval of frequencies in this band, namely for $\omega_{\rm a} \equiv 2\pi \times 3.1$ GHz $< \omega < \omega_p = 2\pi \times 10$ GHz.

Next, by using Eq. (39) and employing the techniques of [28], we reduce Eq. (38) to:

$$\partial_z^2 E - \frac{1-F}{c^2}\partial_t^2 E - \frac{1}{c^2}[F\omega_{\rm res}^2 + (1-F)\omega_p^2]E - \frac{\alpha}{c^2}\left[F\omega_{\rm res}^2 E^3 + (1-F)\partial_t^2 E^3\right] = 0, \qquad (40)$$

where c is the velocity of light in vacuum. Next, we measure time, space, and the field intensity E^2 in units of $\omega_{\rm res}^{-1}$, $v/\omega_{\rm res}$ [where $v = c(1-F)^{-1/2}$], and $|\alpha|^{-1}$, respectively, and express Eq. (40) in dimensionless form:

$$\left(\partial_z^2 - \partial_t^2 - \tilde{\rho}\right)E = s\left(\frac{F}{1-F} + \partial_t^2\right)E^3, \qquad (41)$$

where $s = {\rm sgn}(\alpha) = \pm 1$ for focusing or defocusing nonlinearity, respectively, and $\tilde{\rho} = F/(1-F) + (\omega_p/\omega_{\rm res})^2$. We have assumed above that $(\omega_p/\omega_{\rm res})^2 \gg 1$ in order to ensure the validity of the approximation (39) in a wide sub-interval of the HF band gap. Then, $\tilde{\rho}$ is a large parameter, which suggests that $\tilde{\rho} = \rho/\varepsilon$, where ε is a formal small parameter, and $\rho = \mathcal{O}(1)$. Furthermore, considering propagation of small-amplitude short pulses, we introduce a multiple scale ansatz of the form:

$$E = \varepsilon^{3/2}E_1(T_{\rm HF}, Z_1, \cdots) + \varepsilon^{5/2}E_2(T_{\rm HF}, Z_1, \cdots) + \cdots, \qquad (42)$$

where $T_{\rm HF} = \varepsilon^{-2}(t-z)$ and $Z_n = \varepsilon^n z$ $(n = 1, 2, \cdots)$. Substituting Eq. (42) into Eq. (41), we obtain various equations at different orders of ε. In particular, terms at $\mathcal{O}(\varepsilon^{-5/2})$ cancel, there are no terms at $\mathcal{O}(\varepsilon^{-3/2})$, while terms at $\mathcal{O}(\varepsilon^{-1/2})$, cancel provided that:

$$2\partial_\zeta \partial_{T_{\rm HF}} E_1 + \rho E_1 + s\partial_{T_{\rm HF}}^2 E_1^3 = 0, \qquad (43)$$

where $\zeta \equiv Z_1$. Eq. (43) is the short pulse equation (SPE), which was derived in Ref. [25] in the context of ultra-short pulses propagation in nonlinear silica optical fibers.

B. The low-frequency band gap

The LF gap is defined by $0 < \omega < \omega_{\rm res}$ (see Fig. 1). For $\omega \ll \omega_{\rm res}$ we approximate $\hat{\mu}_L(\omega)$ in Eq. (4) by:

$$\hat{\mu}_L(\omega) \approx \mu_0\left(1 + F\frac{\omega^2}{\omega_{\rm res}^2}\right). \qquad (44)$$

Figure 3 depicts the exact [Eq. (4)] and approximate [Eq. (44)] expressions for $\hat{\mu}_L(\omega)$ in the LF band gap for $F = 0.02$, $\omega_{\rm res} = 2\pi \times 1.45$ GHz. The relative error is less than 5% for $0 < \omega < \omega_{\rm b} \equiv 2\pi \times 1.28$ GHz.

Now, we use Eq. (44) and follow a similar procedure with that of the HF gap, to reduce Eq. (38) to:

$$\partial_z^2 E - \frac{1}{c^2}\left(1 - F\frac{\omega_p^2}{\omega_{\rm res}^2}\right)\partial_t^2 E - \frac{\omega_p^2}{c^2}E = -\frac{F}{\omega_{\rm res}^2 c^2}\partial_t^4 E + \frac{\alpha}{c^2}\partial_t^2 E^3 - \frac{\alpha F}{\omega_{\rm res}^2 c^2}\partial_t^4 E^3. \quad (45)$$

Notice that in Eq. (45), the ratio $(\omega_p/\omega_{\rm res})^2$ is considered to be a $\mathcal{O}(1)$ parameter (as, e.g., in Ref. [24]) since ω_p is not involved in the band width of the LF band gap. In this band, it is convenient to use the filling factor F as the small parameter; this is a physically relevant choice for SRRs [36], as well as for other types of MMs [37].

Next, we measure time, space, and the field intensity E^2 in units of $\omega_{\rm res}^{-1}$, $c/\omega_{\rm res}$ and $|\alpha|^{-1}$, respectively, and thus reduce Eq. (45) to the dimensionless form:

$$\left(\partial_z^2 - \partial_t^2 - \frac{\omega_p^2}{\omega_{\rm res}^2}\right)E = s\partial_t^2 E^3. \quad (46)$$

From Eq. (46), we derive an SPE for the LF band by using the asymptotic expansion:

$$E = \varepsilon E_1(T_{\rm LF}, Z_1, \cdots) + \varepsilon^2 E_2(T_{\rm LF}, Z_1, \cdots) + \cdots, \quad (47)$$

where $T_{\rm LF} = \varepsilon^{-1}(t - z)$ and $Z_n = \varepsilon^n z$ ($n = 1, 2, \cdots$). Substituting Eq. (47) into Eq. (46), the terms at $\mathcal{O}(\varepsilon^{-1})$ cancel, there are no terms at $\mathcal{O}(\varepsilon^0)$, while terms at $\mathcal{O}(\varepsilon)$, cancel provided that E_1 satisfies the SPE:

$$2\partial_\zeta \partial_{T_{\rm LF}} E_1 + \frac{\omega_p^2}{\omega_{\rm res}^2}E_1 + s\partial_{T_{\rm LF}}^2 E_1^3 = 0. \quad (48)$$

C. Solutions of the short pulse equations

We discuss solutions of the SPEs by unifying Eqs. (43) and (48) in the single equation with respect to $u \equiv E_1$:

$$\partial_\zeta \partial_\tau u + \Gamma u + \frac{1}{2}s\partial_\tau^2 u^3 = 0, \quad (49)$$

where $\Gamma = \rho/2$ and $\tau = T_{\rm HF}$ for the HF gap, and $\Gamma = \omega_p^2/(2\omega_{\rm res}^2)$ and $\tau = T_{\rm LF}$ for the LF gap. Seeking travelling wave solutions $u = u(\xi)$, where $\xi = \zeta - C\tau$, Eq. (49) is reduced to the ordinary differential equation:

$$-Cu_{\xi\xi} + \Gamma u + \frac{1}{2}sC^2(6uu_\xi^2 + 3u^2 u_{\xi\xi}) = 0, \quad (50)$$

which by means of the transformation $u_\xi^2 = w(u)$ yields:

$$u_\xi^2 = -\frac{\Gamma u^2}{C}\frac{3sCu^2 - 4}{(3sCu^2 - 2)^2}, \quad (51)$$

subject to the initial condition $u_\xi(\pm\infty) = u(\pm\infty) = 0$ or $w(u(\pm\infty)) = w(0) = 0$. For $sC < 0$ the solutions (51) are always either ascending or descending, while for $sC > 0$ bounded solutions are allowed. In the case $s = +1$ (i.e., focusing dielectrics with $\alpha > 0$), which implies that $C > 0$, the maximum of the travelling wave occurs when $u = \sqrt{4/3C}$. To avoid the singularity at $u = \sqrt{2/3C}$, we consider small amplitude pulses and Eq. (51) is reduced to $u_\xi^2 = (\Gamma/C)u^2$, which possesses a *peakon*-like solution (see, e.g. [38]) of the form:

$$u(\xi) = A\exp(-\sqrt{\Gamma/C}|\xi|), \quad (52)$$

whose derivative has a discontinuity at $\xi = 0$, with amplitude $A < \sqrt{2/3C}$. Also, when the above approximation is not used, the right-hand side of Eq. (51) needs to be positive giving $|u| < \sqrt{4/3|C|}$. These characteristics are consistent with the fact that the SPE exhibits loop-solitons (see [39]).

Moreover, based on the formal connection between the SPE and the sine-Gordon equation (SGE), a smooth, sech-shaped, envelope soliton solution of the SPE, based on the breather solution of the SGE, was derived in [39]. In the framework of Eq. (49), this solution has the form:

$$u \approx \frac{4m}{\sqrt{3\Gamma}}\cos(\zeta + \Gamma\tau)\,\mathrm{sech}\left[m(\zeta - \Gamma\tau)\right], \quad (53)$$

where $0 < m < 1$. The shape of the SPE pulse in Eq. (53) bears resemblance to the NLS soliton, as it consists of a sech-shaped pulse modulating a cos-shaped function. In particular, a connection is established in [28] between the SPE and NLS equations by showing that the envelope function A satisfies the NLS equation:

$$i\left(\partial_{\zeta_2}A + k'\partial_{\tau_2}A\right) - \frac{k''}{2}\partial_{\bar\tau_1}^2 A + \frac{3}{2}\omega|A|^2 A = 0, \quad (54)$$

where $\zeta_n = \varepsilon^n\zeta$, $\tau_n = \varepsilon^n\tau$ ($\varepsilon \ll 1$ and $n = 0, 1, \cdots$), $\bar\tau_1 = \tau_1 - k'\zeta_1$, $k' = -k/\omega$, and $k'' = 2k/\omega^2$. Clearly the well-known sech-shaped envelope soliton solution of the NLS Eq. (54) resembles the soliton of Eq. (53), and scales in space and time similarly. Such smooth SPEs solutions are weak gap solitons that can be formed in the HF and LF band gaps of the nonlinear MM.

D. Numerical simulations

We end up by giving some indicative numerical simulations concerning Eqs. (49) and (41); for further details, analysis and discussions on these

simulations see [28]. The utilized methodology for these simulations relies on Fourier transforming Eq. (49) with respect to τ, then solving the ensuing first order ODE in ζ (for each frequency), via a fourth-order Runge-Kutta scheme, and then Fourier transforming back to obtain $u(\zeta, \tau)$. We use the constant set of parameters $s = 1$, $F = 0.4$, and $\omega_p/\omega_{\rm res} = 10/1.45$ and $\varepsilon = 0.1$. The initial condition is depicted in Fig. 4a and is obtained as the exact breather solution of the SPE equation (Eq. (22) in [39], with $m = 0.32$). The evolution of the breather is shown both in Fig. 4b depicting the contour plot of the space-time evolution as well as in Fig. 4d, depicting the center of mass of the solution vs. time. This is a robust localized structure propagating through the domain with constant speed in time. We have also integrated Eq. (41) with the same type of breather initial profile. In the latter case, however, from the multiple scale ansatz, the initial condition of Eq. (41) was $E(0, \tau) = \varepsilon u(0, \tau)$, $E_z(0, \tau) = -u_\tau(0, \tau)$. The result of the time integration is shown in Fig. 4c. Evidently, the breather is robust in this setting as well, although its propagation speed is slightly smaller than that of the SPE breather. This result confirms our prediction that such "gap breathers" should be observable in the considered type of nonlinear MMs.

V. CONCLUSIONS AND FUTURE WORK

In conclusion, we analyzed electromagnetic (EM) pulse propagation in the left-handed (LH) regime and in the frequency band gaps of nonlinear metamaterials (MMs). In the LH regime, we used the reductive perturbation method to derive from Maxwell's equations a nonlinear Schrödinger (NLS) and a higher-order NLS (HNLS) equation. We found necessary conditions for the formation of bright or dark ultra-short solitons, as well as analytical expressions for these solitons. In the frequency band gaps [with negative (positive) linear permittivity (permeability) hence not allowing propagation of linear EM waves] we derived short-pulse equations (SPEs) describing the propagation of ultra-short pulses. We discussed the structure of the SPEs solutions and presented peakon-like and NLS-like solitons, which can be regarded as weak ultra-short gap solitons. The existence of such structures, indicates the possibility of nonlinear localization of EM waves in the gaps of nonlinear MMs.

Interesting subjects for future research may include a systematic study of the stability and dy-

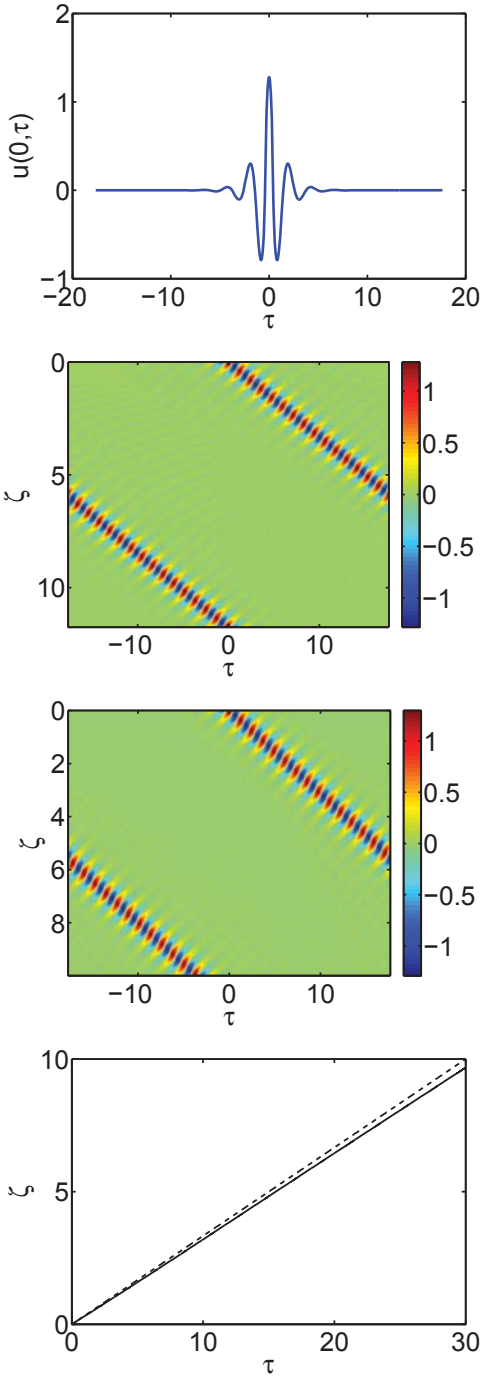

Fig. 4. (a) Breather initial condition used in Eqs. (49) and (41), (b) space-time contour plot of the field evolution in Eq. (49), (c) the same as in (b) but for Eq. (41), (d) evolution of the breathers' center of mass in the two respective models by dotted and solid lines.

namics of the ultra-short or gap solitons, both in the framework of the HNLS or SPE as well as in that of Maxwell's equations. Moreover, it is also worthwhile to analyze the MM in its initial form of conducting wires and SRR's by a suitable CEM methodology (e.g. FDTD or MoM) in order to derive the propagating pulses and then compare them with (i) the solutions of the Maxwell's system (8) after assuming an effective medium approach for the material parameters (see Eqs. (3) and (4)), and (ii) the ultra-short solitons solutions derived in Section III-D. On the other hand, the consideration in the SPE models of the linear losses related to the permittivity and permeability of the MM would result to more general and interesting to investigate SPEs, which would also incorporate first temporal derivative terms of the electric field constituting control mechanisms of the evolution of the gap soliton.

Furthermore, it is highly worthwhile to carry out the corresponding investigations, concerning solitons formation and propagation, in other more complicated types of nonlinear MMs, exhibiting negative refractive index in a certain frequency band. For example, a representative material of this class is an isotropic chiral MM for which one of the two refractive indices can have a negative real part [40,41]; for the EM modelling of linear chiral media see [42], while for applications of negative index chiral MMs see [43]. For a nonlinear chiral MM, application of the reductive perturbation method leads to a system of two coupled NLS equations for the LH and RH Beltrami components of the EM field. For a sufficiently large chirality parameter there exists a certain spectral regime where the refractive index for the LH/RH Beltrami component is real and negative but that for the RH/LH Beltrami component is real and positive [40]. To this direction, it is interesting to approximate, inside the above regime, the coupled system of the NLS equations by a completely integrable system, and hence predict various classes of exact vector soliton solutions (bright-bright, dark-dark, as well as dark-bright solitons) that can be supported in the nonlinear chiral MM. Certain relevant investigations are reported in [44].

ACKNOWLEDGMENT

The author thanks sincerely Dimitri J. Frantzeskakis for the introduction to this field and for the valuable encouragement throughout this research.

REFERENCES

[1] G. V. Eleftheriades and K. G. Balmain, *Negative-Refraction Metamaterials. Fundamental Principles and Applications*, John Wiley, New Jersey, 2005.

[2] C. Caloz and T. Itoh, *Electromagnetic Metamaterials. Transmission Line Theory and Microwave Applications*, John Wiley, New Jersey, 2006.

[3] D. R. Smith, W. J. Padilla, D. C. Vier, S. C. Nemat-Nasser, and S. Schultz, "Composite Medium with Simultaneously Negative Permeability and Permittivity," *Phys. Rev. Lett.*, vol. 84, pp. 4184-4187, May 2000.

[4] A. Shelby, D. R. Smith, and S. Schultz, "Experimental Verification of a Negative Index of Refraction," *Science*, vol. 292, pp. 77-79, Apr. 2001.

[5] M. C. Tang, S. Q. Xiao, D. Wang, J. Xiong, K. Chen, and B. Z. Wang, "Negative Index of Reflection in Planar Metamaterial Composed of Single Split-Ring Resonators," *ACES J.*, vol. 26, pp. 250-258, Mar. 2011.

[6] V. Shalaev, "Optical Negative-Index Metamaterials," *Nature Photonics*, vol. 1, pp. 41-48, Jan. 2007.

[7] V. G. Veselago, "Electrodynamics of Substances with Simultaneously Negative Values of Sigma and Mu," *Sov. Phys. Usp.*, vol. 10, pp. 509, 1968.

[8] J. B. Pendry, "Negative Refraction Makes a Perfect Lens," *Phys. Rev. Lett.*, vol. 85, pp. 3966-3969, Oct. 2000.

[9] D. R. Smith, J. B. Pendry, and M. C. K. Wiltshire, "Metamaterials and Negative Refractive Index," *Science*, vol. 305, pp. 788-792, Aug. 2004.

[10] J. B. Pendry and D. R. Smith, "Reversing Light with Negative Refraction," *Phys. Today*, vol. 57, pp. 37-43, Jun. 2004.

[11] S. A. Ramakrishna, "Physics of Negative Refractive Index Materials," *Rep. Prog. Phys.*, vol. 68, pp. 449-521, Feb. 2005.

[12] C. M. Soukoulis, M. Kafesaki, and E. N. Economou, "Negative-Index Materials: New Frontiers in Optics," *Adv. Materials*, vol. 18, pp. 1941-1952, Aug. 2006.

[13] J. C. Liu, W. Shao, and B. Z. Wang, "A Dual-Band Metamaterial Design using Double SRR Structures," *ACES J.*, vol. 26, pp. 459-463, Jun. 2011.

[14] Y. Huang, G. Wen, T. Li, and K. Xie, "Positive-Negative-Positive Metamaterial Consisting of Ferrimagnetic Host and Wire Array," *ACES J.*, vol. 25, pp. 696-702, Aug. 2010.

[15] G. Antonini, "Reduced Order Models for Metamaterial Transmission Lines," *ACES Newsletter*, vol. 21, pp. 78-103, 2006.

[16] A. A. Zharov, I. V. Shadrivov, and Yu. S. Kivshar, "Nonlinear Properties of Left-Handed Metamaterials," *Phys. Rev. Lett.*, vol. 91, 037401, Jul. 2003.

[17] V. M. Agranovich, Y. R. Shen, R. H. Baughman, and A. A. Zakhidov, "Linear and Nonlinear Wave Propagation in Negative Refraction Metamaterials," *Phys. Rev. B*, vol. 69, 165112, Apr. 2004.

[18] N. Lazarides and G. P. Tsironis, "Coupled Nonlinear Schrödinger Field Equations for Electromagnetic Wave Propagation in Nonlinear Left-Handed Materials," *Phys. Rev. E*, vol. 71, 036614, Mar. 2005.

[19] I. V. Shadrivov, A. A. Zharov, N. A. Zharova, and Yu. S. Kivshar, "Nonlinear Left-Handed Metamaterials," *Radio Science*, vol. 40, RS3S90, May 2005.

[20] M. Scalora, M. S. Syrchin, N. Akozbek, E. Y. Poliakov, G. D'Aguanno, N. Mattiucci, M. J. Bloemer, and A. M. Zheltikov, "Generalized Nonlinear Schrodinger Equation for Dispersive Susceptibility and Permeability: Application to Negative Index Materials," *Phys. Rev. Lett.*, vol. 95, 013902, Jul. 2005.

[21] S. C. Wen, Y. J. Xiang, X. Y. Dai, Z. X. Tang, W. H. Su, and D. Y. Fan, "Theoretical Models for Ultrashort Electromagnetic Pulse Propagation in Nonlinear Metamaterials," *Phys. Rev. A*, vol. 75, 033815, Mar. 2007.

[22] I. V. Shadrivov and Yu. S. Kivshar, "Spatial Solitons in Nonlinear Left-Handed Metamaterials," *J. Opt. A: Pure Appl. Opt.*, vol. 7, pp. S68-S72, Feb. 2005.

[23] A. Aceves, "Optical Gap Solitons: Past, Present, and Future; Theory and Experiments," *Chaos*, vol. 10, pp. 584-589, Sep. 2000.

[24] S. Longhi, "Gap Solitons in Metamaterials," *Waves in Random and Complex Media*, vol. 15, pp. 119-126, Feb. 2005.

[25] T. Schäfer and C. E. Wayne, "Propagation of Ultra-Short Optical Pulses in Cubic Nonlinear Media," *Physica D*, vol. 196, pp. 90-105, Sep. 2004.

[26] N. Costanzino, V. Manukian, and C. K. R. T. Jones, "Solitary Waves of the Regularized Short Pulse and Ostrovsky Equations," *SIAM J. Math. Anal.*, vol. 41, pp. 2088-2106, 2009.

[27] N. L. Tsitsas, N. Rompotis, I. Kourakis, P. G. Kevrekidis, and D. J. Frantzeskakis, "Higher-Order Effects and Ultrashort Solitons in Left-Handed Metamaterials," *Phys. Rev. E*, vol. 79, 037601, Mar. 2009.

[28] N. L. Tsitsas, T. P. Horikis, Y. Shen, P. G. Kevrekidis, N. Whitaker, and D. J. Frantzeskakis, "Short Pulse Equations and Localized Structures in Frequency Band Gaps of Nonlinear Metamaterials," *Phys. Let. A*, vol. 374, pp. 1384-1388, Mar. 2010.

[29] I. Kourakis and P. K. Shukla, "Nonlinear Propagation of Electromagnetic Waves in Negative-Refraction-Index Composite Materials," *Phys. Rev. E*, vol. 72, 016626, Jul. 2005.

[30] T. Taniuti, "Reductive Perturbation Method and Far Fields of Wave-Equations," *Prog. Theor. Phys. Suppl.*, vol. 55, pp. 1-35, 1974.

[31] Y. Kodama and A. Hasegawa, "Nonlinear Pulse-Propagation in a Monomode Dielectric Guide," *IEEE J. Quantum Electron.*, vol. 23, pp. 510-524, May 1987.

[32] A. Hasegawa and Y. Kodama, *Solitons in Optical Communications*, Clarendon Press, Oxford, 1995.

[33] J. V. Moloney and A. C. Newell, *Nonlinear Optics*, Westview Press, Oxford, 2004.

[34] G. P. Agrawal, *Nonlinear Fiber Optics*, Academic Press, London, 2007.

[35] K. Hizanidis, D. J. Frantzeskakis, and C. Polymilis, "Exact Travelling Wave Solutions for a Generalized Nonlinear Schrodinger Equation," *J. Phys. A: Math. Gen.*, vol. 29, pp. 7687-7703, Dec. 1996.

[36] L. Kang, Q. Zhao, H. Zhao, and J. Zhou, "Magnetically Tunable Negative Permeability Metamaterial Composed by Split Ring Resonators and Ferrite Rods," *Opt. Express*, vol. 16, pp. 8825-8834, Jun. 2008.

[37] S. Zhang, W. Fan, K. J. Malloy, S. R. J. Brueck, N. C. Panoiu, and R. M. Osgood, "Near-Infrared Double Negative Metamaterials," *Opt. Express*, vol. 13, pp. 4922-4930, Jun. 2005.

[38] R. Camassa and D. D. Holm, "An Integrable Shallow-Water Equation with Peaked Solitons," *Phys. Rev. Lett.*, vol. 71, pp. 1661-1664, Sep. 1993.

[39] A. Sakovich and S. Sakovich, "Solitary Wave Solutions of the Short Pulse Equation," *J. Phys. A: Math. Gen.*, vol. 39, pp. L361-L367, Jun. 2006.

[40] T. G. Mackay and A. Lakhtakia, "Plane Waves with Negative Phase Velocity in Faraday Chiral Mediums," *Phys. Rev. E*, vol. 69, 026602, Feb. 2004.

[41] J. B. Pendry, "A Chiral Route to Negative Refraction," *Science*, vol. 306, pp. 1353-1355, Nov. 2004.

[42] V. Demir, A. Z. Elsherbeni, and E. Arvas, "FDTD Formulation for Dispersive Chiral Media using the Z Transform Method," *IEEE Trans. Antennas Propagat.*, vol. 53, pp. 3374-3384, Oct. 2005.

[43] N. Wongkasem, A. Akyurtlu, K. A. Marx, Q. Dong, J. Li, and W .D. Goodhue, "Development of Chiral Negative Refractive Index Metamaterials for the Terahertz Frequency Regime," *IEEE Trans. Antennas Propagat.*, vol. 55, pp. 3052-3062, Nov. 2007.

[44] N. L. Tsitsas, A. Lakhtakia, and D. J. Frantzeskakis, "Vector Solitons in Nonlinear Isotropic Chiral Metamaterials," *J. Phys. A: Math. Theor.*, vol. 44, 435203, Oct. 2011.

Nikolaos L. Tsitsas was born in Athens, Greece, in 1979. He received the Diploma and Ph.D. Degree in Electrical Engineering from the National Technical University of Athens (NTUA) in 2002 and 2006 respectively, and the M.Sc. Degree in Applied Mathematics from the National and Kapodistrian University of Athens in 2005.

From 2008 to 2011, he was an Adjunct Lecturer at the School of Applied Mathematical and Physical Sciences of the NTUA. From 2009 to 2011, he was an Adjunct Lecturer at the Hellenic Army Academy. Since 2012, he has been an Assistant Professor at the Department of Informatics of the Aristotle University of Thessaloniki. He is the author or coauthor of 30 papers in scientific journals and 36 papers in conference proceedings. His research interests include analytical and numerical methods in direct and inverse wave scattering and propagation theory as well as numerical solution techniques of integral and partial differential equations.

Dr. Tsitsas is a member of the IEEE, the Optical Society of America, the American Mathematical Society, and the Technical Chamber of Greece.